

Research Article

# The Heilongjiang Group: A Jurassic accretionary complex in the Jiamusi Massif at the western Pacific margin of northeastern China

FU-YUAN WU,<sup>1\*</sup> JIN-HUI YANG,<sup>1</sup> CHING-HUA LO,<sup>2</sup> SIMON A. WILDE,<sup>3</sup> DE-YOU SUN<sup>4</sup> AND BOR-MING JAHN<sup>5</sup>

<sup>1</sup>State Key Laboratory of Lithospheric Evolution, Institute of Geology and Geophysics, Chinese Academy of Sciences, PO Box 9825, Beijing 100029, China (email: wufuyuan@mail.igcas.ac.cn), <sup>2</sup>Department of Geology, National Taiwan University, Taipei, Taiwan, China, <sup>3</sup>Department of Applied Geology, Curtin University of Technology, Perth, Western Australia, Australia, <sup>4</sup>College of Earth Sciences, Jilin University, Changchun, China and <sup>5</sup>Institute of Earth Sciences, Academia Sinica, Nankang, Taipei, Taiwan, China

**Abstract** The tectonic setting of the Eastern Asian continental margin in the Jurassic is highly controversial. In the current study, we have selected the Heilongjiang complex located at the western margin of the Jiamusi Massif in northeastern China for geochronological investigation to address this issue. Field and petrographic investigations indicate that the Heilongjiang complex is composed predominately of granitic gneiss, marble, mafic-ultramafic rocks, blueschist, greenschist, quartzite, muscovite-albite schist and two-mica schist that were tectonically interleaved, indicating they represent a *mélange*. The marble, two-mica schist and granitic gneiss were most probably derived from the Mashan complex, a high-grade gneiss complex in the Jiamusi Massif with which the Heilongjiang Group is intimately associated. The ultramafic rocks, blueschist, greenschist and quartzite (chert) are similar to components in ophiolite. The sensitive high mass-resolution ion microprobe U-Pb zircon age of  $265 \pm 4$  Ma for the granitic gneiss indicates that the protolith granite was emplaced coevally with Permian batholiths in the Jiamusi Massif. <sup>40</sup>Ar/<sup>39</sup>Ar dating of biotite and phengite from the granitic gneiss and mica schist yields a late Early Jurassic metamorphic age between 184 and 174 Ma. Early components of the Jiamusi Massif, including the Mashan complex, probably formed part of an exotic block from Gondwana, affected by late Pan-African orogenesis, and collided with the Asian continental margin during the Early Jurassic. Subduction of oceanic crust between the Jiamusi block and the eastern part of the Central Asian Orogenic Belt resulted in the formation of a huge volume of Jurassic granites in the Zhangguangcai Range. Consequently, the collision of the Jiamusi Massif with the Central Asian Orogenic Belt to the west can be considered as the result of circum-Pacific accretion, unrelated to the Central Asian Orogenic Belt. The widespread development of Jurassic accretionary complexes along the Asian continental margin supports such an interpretation.

**Key words:** Heilongjiang complex, Jiamusi Massif, Jurassic subduction, northeastern China, ophiolite.

## INTRODUCTION

In recent years, geochronological studies in northeastern China have identified large volumes of

Mesozoic granites (Wu *et al.* 2000, 2001b, 2002, 2003; Zhang *et al.* 2004). In the Zhangguangcai Range of eastern Heilongjiang and Jilin provinces, more than 90% of the approximate 100 000 km<sup>2</sup> of granites were emplaced between 205 and 155 Ma in the Jurassic period (Wu *et al.* 2000), not in the Paleozoic as previously thought.

\*Correspondence.

Received 18 February 2005; accepted for publication 19 July 2006.

Jurassic granites (often referred to as 'Early Yanshanian' in Chinese published reports) are also widely developed in other areas of eastern Asia, including the Liaodong and Jiaodong Peninsulas in northeastern China, the Korean Peninsula and also in southeastern China (Wang *et al.* 1998; Chough *et al.* 2000; Zhou & Li 2000; Sagong *et al.* 2005; Wu *et al.* 2005). In southeastern China, Jurassic granites occupy approximately 50% of the total area of ~200 000 km<sup>2</sup>.

The geodynamic setting in which these Jurassic granites formed, however, is still controversial. Commonly, they are regarded as being generated at an active continental margin related to subduction of the Kula or Izanagi Plate under Eurasia, leading to the development of calc-alkaline magmatism (Takahashi 1983; Natal'in & Borukayev 1991; Natal'in 1991; Faure & Natal'in 1992; Faure *et al.* 1995; Gilder *et al.* 1996; Zhou & Li 2000; Deng *et al.* 2004). However, this model has been criticized in that the width of the contemporaneous magmatic arc (>1000 km) is far greater than that normally observed in subduction-related environments, although it has been suggested that later strike-slip movement might change the position of the original subduction zone (Sengör & Natal'in 1996). Furthermore, recent studies conducted in southeastern China indicate the occurrence of coeval A-type granites and intraplate basaltic rocks (Chen *et al.* 2002; Li *et al.* 2003; Fu *et al.* 2004), suggesting development in an extensional setting. In the current study, we present sensitive high mass-resolution ion microprobe (SHRIMP) and inductively coupled plasma-mass spectrometry (ICP-MS) U-Pb zircon and <sup>40</sup>Ar/<sup>39</sup>Ar mica geochronologic data for the Heilongjiang complex, a blueschist-facies ophiolitic mélange in northeastern China. The timing of assembly and its relations to other components of the Jiamusi Massif will enable evaluation of the timing and mechanism of accretion along the northwest Pacific margin.

## GEOLOGICAL SETTING

### REGIONAL CONTEXT

Northeastern China has traditionally been considered as the eastern part of the Paleozoic Central Asian Orogenic Belt (CAOB), located between the Siberian and North China cratons (Sengör *et al.* 1993; Jahn *et al.* 2000; Jahn 2004; Li 2006). It consists of a collage of several microcontinental blocks (Ye *et al.* 1994; Wu *et al.* 1995): the Jiamusi Massif

(block) in the southeast, the Songliao block in the middle, and the Xing'an and Erguna blocks in the northwest, separated by the Mudanjiang, Hegenshan-Nenjiang and Tayuan-Xiguitu Faults (Fig. 1).

The Jiamusi Massif contains three different rock series: the Mashan complex, the Heilongjiang complex and Early and Late Paleozoic granitoids. The Mashan complex is characterized by khondalitic series rocks (granulite, marble, graphitic schist), metamorphosed to granulite facies. It was traditionally considered to be Late Archean in age (HBGMR 1993), but recent SHRIMP dating and isotopic investigations showed that metamorphism took place in the early Paleozoic at *ca* 500 Ma (Wilde *et al.* 1997; Wilde *et al.* 2000), with Nd model ages less than 2.0 Ga (Jahn, unpubl. data, 2005). Two stages of granitoids have been identified: the metamorphosed and deformed granitoids associated with the Mashan complex have been identified as representing Late Pan-African granitic magmatism in the area with an emplacement age of *ca* 520 Ma (Wilde *et al.* 2003), whereas the Permian granites show weakly to un-deformed structure (Wilde *et al.* 1997; Wu *et al.* 2000). The Heilongjiang complex, the subject of the present study, is discussed in more detail below.

The Songliao block is mostly restricted by the Songliao Sedimentary Basin. Its eastern and northern parts are the Zhangguangcai and Lesser Xing'an Ranges, which are characterized by voluminous Mesozoic granitic rocks with rare Paleozoic strata occurring as remnants in a 'sea' of granite (Wu *et al.* 2000). Recent borehole data from the Songliao Basin show that granites are widespread and form the basement (Wu *et al.* 2001b). The Xing'an block, located in the Great Xing'an Range, is characterized by extensive Mesozoic volcanic and granitic rocks, although some are now known to have formed in the Paleozoic (Wu *et al.* 2002; Fan *et al.* 2003; Ge *et al.* 2005b), whereas Paleozoic strata are well developed in the southern part. Proterozoic metamorphic rocks had previously been identified (HBGMR 1993), but recent geochronologic work indicates they are in fact Paleozoic in age (Miao *et al.* 2004). The Erguna block, considered to be the eastern extension of the Central Mongolian microcontinent, is located in the northwestern part of the region (Fig. 1). Its geological evolution is largely unknown as the region is heavily forested. This block is characterized by the presence of Proterozoic to Paleozoic strata and granites (HBGMR 1993), but few reliable geochronologic data are available. Recent work indicates that the Early

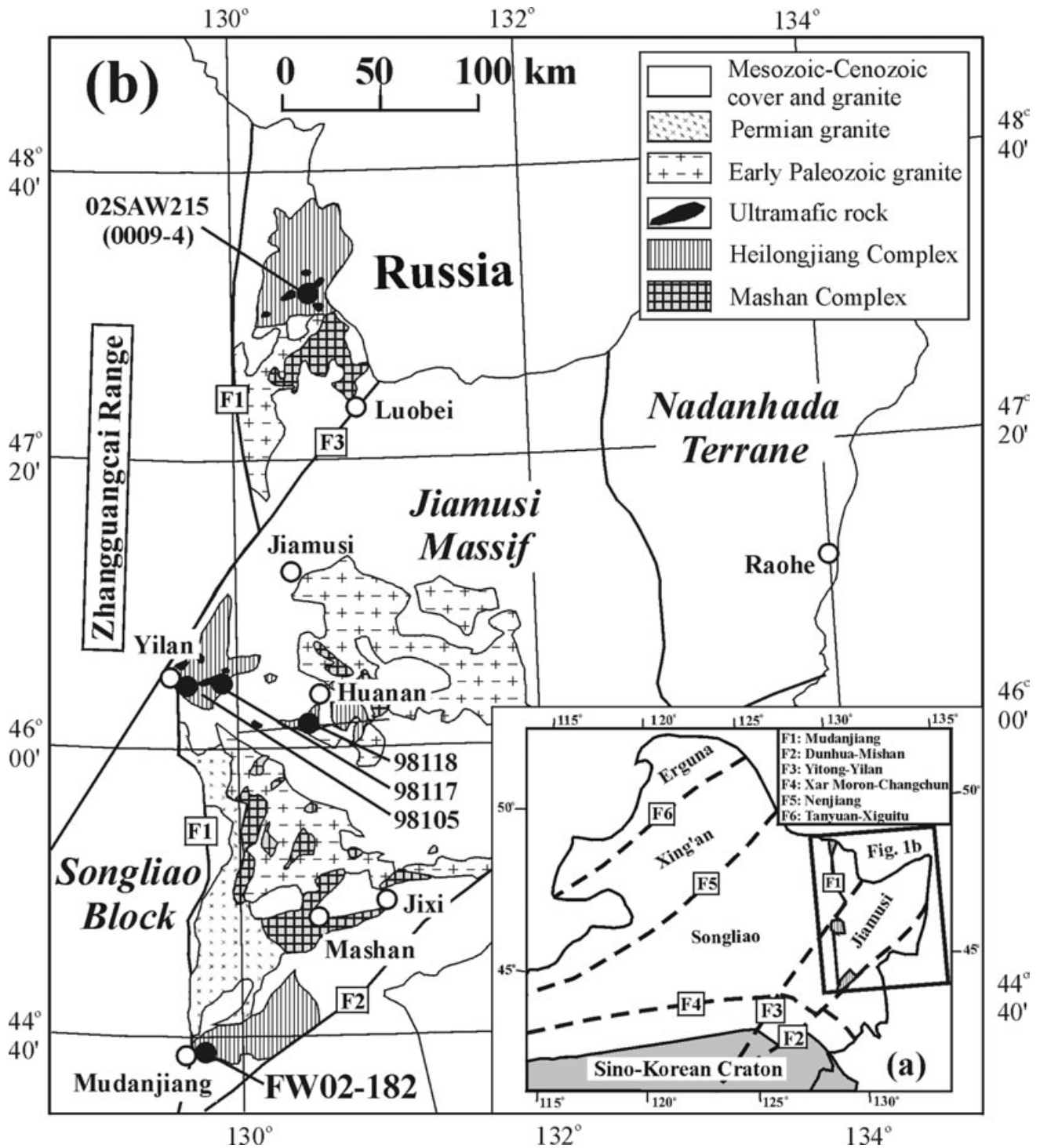


**Fig. 1** Simplified geological map of (a) northeastern China and (b) the Jiamusi Massif (modified from Wilde *et al.* 1997). The Songliao block, located to the west, is characterized by Early–Middle Jurassic granites in the Zhanguangcai Range. F1: Mudanjiang Fault, F2: Dunhua-Mishan Fault, F3: Yitong-Yilan Fault, F4: Xra Moron-Changchun Fault, F5: Hegenshan-Nenjiang, F6: Tanyuan-Xiguitu Fault.

Paleozoic granitic magmatism is well developed in the area (Ge *et al.* 2005a).

**HEILONGJIANG COMPLEX**

According to regional geological surveys by the HBGMR (1993) and Cao *et al.* (1992), the

Heilongjiang complex is exposed in three main areas; around Luobei in the north, near Yilan in the central part and around Mudanjiang in the south, close to the Mudanjiang Fault (Fig. 1). It was initially considered that the Heilongjiang complex represented a Proterozoic stratigraphic

sequence in the Jiamusi Massif and was termed the Heilongjiang Group by HBGM (1993). Cao *et al.* (1992) proposed that the Heilongjiang is an accretionary complex formed in the Silurian between the Jiamusi and Songliao blocks.

The exact distribution of various rocks in the Heilongjiang complex has not been fully investigated, because of the limited exposure beneath heavy forest. In the Lubei area, the main rock types include blueschist, greenschist, marble, serpentinite and quartzite with an ENE-directed foliation. It is noted that granitic gneiss and graphite-bearing marble of the Mashan complex has been juxtaposed within the Heilongjiang complex in this area. At Yilan, the Heilongjiang complex is characterized by the occurrence of serpentinite, blueschist, greenschist, two-mica schist, muscovite-albite schist and quartz schist (quartzite). The serpentinite occurs locally and is in tectonic contact with other rocks; the residual minerals indicate that the ultramafic protoliths include dunite, lherzolite and harzburgite. Sillimanite, garnet and graphite in the two-mica schists indicate derivation from the Mashan complex. In the greenschist and muscovite-albite schist, crossite with rims of barroisite and winchite commonly occurs in albite porphyroblasts. Magneisoriebeckite has also been identified. All of these clearly indicate that some of the Heilongjiang complex has undergone blueschist facies high-pressure metamorphism. At Mudanjiang, the Heilongjiang complex is exposed in a series of tectonic slices and is composed of two-mica schist, greenschist and blueschist with minor serpentinite, quartzite and marble. The two-mica schist is fine-grained and shows an intense mylonitic fabric. Locally, stratigraphic layering indicates a sedimentary origin (Cao *et al.* 1992; Li *et al.* 1999). Blueschists commonly preserve pillow structures. Geochemical analyses by Li *et al.* (1999) suggest the greenschist and blueschist represent metamorphosed tholeiitic and alkaline basalts, respectively, the tholeiite formed at a spreading center and the alkali basalt in an intra-oceanic setting. The quartzite is associated with greenschist and Fe-Mn nodules (pyrolusite and psilomelane), with spessartine, stilpnomelane, sodium-amphibole and piemontite, indicating its deposition in an abyssal setting (Li *et al.* 1999).

In summary, the major rock types of the Heilongjiang complex show a large variation. All of these rocks have undergone greenschist to blueschist facies metamorphism, accompanied by intense deformation. A brief description of the key rock units is presented below.

1. Granitic gneiss is characterized by the presence of porphyroclastic plagioclase showing various degrees of deformation. The mineral assemblage is quartz, plagioclase, hornblende, muscovite, biotite and K-feldspar.
2. Two-mica schist is mostly medium-grained and the mineral assemblage is muscovite, biotite, quartz, K-feldspar, garnet and sillimanite. It locally grades into muscovite-quartz schist when there is less biotite.
3. Muscovite-albite schist is strongly foliated and composed of quartz, albite, muscovite, garnet, epidote and stilpnomelane (but without biotite). Barroisite inclusions are not uncommon in porphyroblastic albite.
4. Quartzite is considered to be deformed and metamorphosed chert, composed of quartz, stilpnomelane, epidote, spessartine, piemontite, pyrolusite and psilomelane (Cao *et al.* 1992).
5. Marble is mainly exposed near Luobei, and also occurs in the nearby Mashan complex. In some locations, marble is associated with ultramafic rocks. However, it also occurs with quartzite (chert), indicating its association with abyssal sedimentary rocks.
6. For the blueschist and greenschist, two stages of mineral growth have been identified (Yan *et al.* 1989; Cao *et al.* 1992), although the rocks have undergone extensive deformation. The first stage is characterized by the occurrence of crossite + barroisite, indicating blueschist facies metamorphism. The second stage consists of epidote + chlorite + calcite + actinolite + quartz + albite + phengite, and is characteristic of greenschist facies metamorphism. It is therefore suggested that metamorphic pressure decreased through time. Although intensively deformed, pillow structures can still be observed in the field, indicating the subaqueous eruption of the protolith.
7. Mafic-ultramafic rocks occur as tectonic lenses and slices within mylonitized granite, muscovite-albite schist and marble. The major rock types include serpentinitized lherzolite, pyroxenite and gabbro (Yan *et al.* 1989; HBGM 1993). It is evident that the Heilongjiang complex is composed of a variety of rocks that are tectonically juxtaposed, indicating their possible association in a mélangé. The ultramafic rocks, greenschist, blueschist, albite mica-schist and quartzite (chert) are similar to those commonly found in ophiolite, although the proportion of basalts and ultramafic rocks cannot be estimated because of the poor

exposure (Cao *et al.* 1992; Li *et al.* 1999). Some marbles and coarser two-mica schist might be formed in shallow water at a passive continental margin (Li *et al.* 1999). In addition, granitic gneiss in the Heilongjiang complex is most likely a component of the Mashan complex, incorporated into the Heilongjiang complex during later deformation.

## ANALYTICAL TECHNIQUES

Zircon crystals were extracted from the rock samples by crushing and heavy liquid separation. For the SHRIMP analyses, the individual crystals were hand picked and mounted, along with several pieces of the Curtin University standard (CZ3, which has a conventionally measured  $^{206}\text{Pb}/^{238}\text{U}$  age of 564 Ma [Pidgeon *et al.* 1994]), onto double-sided adhesive tape and enclosed in epoxy resin discs. The discs were polished, so as to effectively section the zircons in half, and then gold coated.

Zircon SHRIMP U-Th-Pb analyses were carried out using the SHRIMP II ion microprobe (Australian Scientific Instruments, Australia) at Curtin University, following standard procedures described by Nelson (1997) and Williams (1998). Spot size ranged between 20 and 30  $\mu\text{m}$  and each analysis spot was rastered over 120  $\mu\text{m}$  for 3 min before analysis to remove any common Pb on the surface or contamination from the gold coating. The mass resolution used to measure Pb/Pb and Pb/U isotopic ratios was 5060 during the analytical session and the Pb/U ratios were normalized to those measured on the standard zircon (CZ3 – [ $^{206}\text{Pb}/^{238}\text{U} = 0.0914$ ]). The error associated with the measurement of Pb/U isotopic ratios for the standard, at 1 standard deviation, was 1.99%. The measured  $^{204}\text{Pb}$  values in the unknowns were similar to those recorded for the standard zircon and so common lead corrections were made assuming an isotopic composition of Broken Hill lead, because the common lead is considered to be mainly associated with surface contamination in the gold coating (Nelson 1997). The  $^{206}\text{Pb}/^{238}\text{U}$  ages are considered to be the most reliable for concordant Phanerozoic zircons (Compston *et al.* 1992). Data reduction was calculated with the Krill 007 program (written by P.D. Kinny, Curtin University of Technology, Australia), applying the  $^{208}\text{Pb}$  correction, because there is no evidence of postcrystallization disturbance to the U-Pb-Th systems of these zircons. Errors on individual analyses are quoted at the  $1\sigma$  level, whereas the error on the pooled analyses is quoted at  $2\sigma$  or 95% confidence.

Detrital zircons were analysed by the laser ablation ICPMS (LA-ICPMS) method. Experiments were carried out at the LA-ICP-MS laboratory of North-west University in Xi'an, using an Elan 6100 Dynamic Reaction Cell ICP-MS from Perkin Elmer/SCIEX (Perkin Elmer, Massachusetts, USA). The instrument allows a sensitivity of approximately 90 million counts per second (cps) for 1  $\mu\text{g}/\text{mL}$  in standard solution nebulization mode (Meinhard concentric nebulizer and cyclonic spray chamber). Background intensities are usually a few cps for elements above  $m/z = 85$  (Rb), except Sn and Pb, which can reach 100–200 cps as a result of memory effect. The GeoLas 200 M laser-ablation system (MicroLas, Göttingen, Germany) was used for laser ablation. The system is equipped with a 193 nm ArF-excimer laser and a homogenizing, imaging optical system. The set-up delivers a flat top beam onto the sample surface and the laser wavelength and energy density (40 J/cm<sup>2</sup>) allows controlled ablation of highly transparent samples. The spot size can be varied between 4 and 120  $\mu\text{m}$  by means of an aperture system, which provides a constant energy density at the ablation site for variable spot sizes, although only 30  $\mu\text{m}$  spot size was adopted in the current study. Helium was used as a carrier gas to enhance transport efficiency of ablated material. Both standards and samples were arranged on the gas line to improve transfer efficiency and reduce elemental fractionation. All the gas lines were purged for over 1 h before each analytical session to remove Pb on the gas line surface to  $^{204}\text{Pb} < 50$  cps in the gas blank. The measurements were carried out using time resolved analysis operating in a fast, peak hopping sequence in dual detector mode. Raw count rates for  $^{29}\text{Si}$ ,  $^{204}\text{Pb}$ ,  $^{206}\text{Pb}$ ,  $^{207}\text{Pb}$ ,  $^{208}\text{Pb}$ ,  $^{232}\text{Th}$  and  $^{238}\text{U}$  were collected for age determination.  $^{202}\text{Hg}$  is usually  $< 10$  cps in the gas blank, therefore the contribution of  $^{204}\text{Hg}$  to  $^{204}\text{Pb}$  is negligible and is not considered further. The integration time for the four Pb isotopes was 62.76 ms, whereas for the other isotopes (including  $^{29}\text{Si}$ ,  $^{232}\text{Th}$  and  $^{238}\text{U}$ ) it was 30 ms. Data were acquired over 30 s with the laser off and 40 s with the laser on, giving approximately 340 (=170 reading/replicate  $\times 2$  sweeps) mass scans for a penetration depth of approximately 20  $\mu\text{m}$ . The averaged gas blank is typically  $< 4000$  cps for  $^{29}\text{Si}$ ;  $< 10$  cps for  $^{204}\text{Pb}$ ,  $^{206}\text{Pb}$ ,  $^{207}\text{Pb}$  and  $^{208}\text{Pb}$ ;  $< 1$  cps for  $^{232}\text{Th}$  and  $^{238}\text{U}$ . U, Th and Pb concentrations were calibrated by using  $^{29}\text{Si}$  as an internal standard and NIST SRM 610 as the external standard.  $^{207}\text{Pb}/^{206}\text{Pb}$  and  $^{206}\text{Pb}/^{238}\text{U}$  ratios were calculated using the GLITTER 4.0 program

(Geochemical Evolution and Metallogeny of Continents, Macquarie University, Sydney, Australia) (Jackson *et al.* 2004), which was then corrected using the Harvard zircon 91 500 as external standard. The  $^{207}\text{Pb}/^{235}\text{U}$  ratio was calculated from the values of  $^{207}\text{Pb}/^{206}\text{Pb}$  and  $^{206}\text{Pb}/^{238}\text{U}$ . Common Pb was corrected according to the method proposed by Andersen (2002). Detailed analytical protocols can be found in Yuan *et al.* (2004).

Rb-Sr isotopic data were obtained at the Institute of Geology and Geophysics, Chinese Academy of Science, using a multicollector VG 354 mass spectrometer (VG Analytical, UK) in static mode. The  $^{87}\text{Sr}/^{86}\text{Sr}$  ratios were normalized against the value of  $^{86}\text{Sr}/^{88}\text{Sr} = 0.1194$ . During the period of data acquisition, standard samples NBS981 and NBS607 gave  $^{87}\text{Sr}/^{86}\text{Sr}$  ratios of  $0.710255 \pm 14$  ( $2\sigma$ ) and  $1.20032 \pm 28$  ( $2\sigma$ ), respectively. Analytical precision of  $^{87}\text{Rb}/^{86}\text{Sr}$  is generally better than 2%.

Samples analyzed for  $^{40}\text{Ar}/^{39}\text{Ar}$  were irradiated in the VT-C position at the THOR reactor in Taiwan for 30 h. To monitor the neutron flux in the reactor, aliquots of the LP-6 standard were stacked along with the samples in each irradiation. Standards and samples were either incrementally heated or totally fused using a double-vacuum resistance furnace and/or a US LASER Nd-YAG laser (New Wave, CA, USA) operated in continuous mode, and the gas was measured by a VG-3600 mass spectrometer at the National Taiwan University. The details of analytical methods are outlined in Lo *et al.* (2002). The  $J$ -values were calculated using argon compositions of the LP-6 biotite standard with a  $^{40}\text{Ar}/^{39}\text{Ar}$  age of  $128.4 \pm 0.2$  Ma (Renne *et al.* 1998). Ages were calculated from Ar isotope ratios measured after corrections made for mass discrimination, interfering nuclear reactions, decays of radiometric isotopes, procedural blanks and atmospheric Ar contamination. Total gas ages were calculated from the sum total of the argon compositions of all the temperature steps. Plateau dates were calculated by the same approach, but using only adjacent temperature steps yielding dates which are concordant with each other within  $2\sigma$ . Data were further plotted on age spectra and  $^{36}\text{Ar}/^{40}\text{Ar}$ – $^{39}\text{Ar}/^{40}\text{Ar}$  isotope correlation diagrams. The intercept dates and  $^{40}\text{Ar}/^{36}\text{Ar}$  intercept values were calculated from the intercept of the regressed line. The cubic least-square fitting method was used in regressing the data. Because the  $^{39}\text{Ar}_K$ ,  $^{38}\text{Ar}_{Cl}$  and  $^{37}\text{Ar}_{Ca}$  release data potentially reflect the chemical compositions (K, Cl and Ca, respectively) of the samples, Ca/K and Cl/K ratios were calculated according to the relationships

$\text{Ca}/\text{K} = 3.32 (\pm 0.17) \times ^{37}\text{Ar}_{Ca}/^{39}\text{Ar}_K$  and  $\text{Cl}/\text{K} = 0.22 (\pm 0.04) \times ^{38}\text{Ar}_{Cl}/^{39}\text{Ar}_K$ , obtained from the analyses of irradiated salts.

U-Pb zircon ICP-MS, Rb-Sr whole-rock isochron and Ar-Ar ages were calculated using the regression program ISOPLOT (Ludwig 1999), and the errors quoted in age computation represent  $\pm 2$  standard deviations. However, the ages of Ar-Ar results are at  $1\sigma$ . All the geochemical data are available from the authors on request.

## SAMPLE DETAILS AND RESULTS

### LUOBEI AREA

Granitic gneiss sample 00SAW215 (0009-4) is a porphyritic dioritic gneiss (the same rock sample, but given different sample numbers) collected from Luobei. The sample is coarse-grained with plagioclase phenocrysts and consists of quartz, plagioclase, biotite and garnet. It is metamorphosed to greenschist-amphibolite facies and has a deformation fabric, defined by aligned biotite. The SHRIMP U-Pb zircon analytical results are presented in Figure 2. The  $^{206}\text{Pb}/^{238}\text{U}$  weighted mean age of all 12 analyses is  $256 \pm 7$  Ma. In detail, the zircons can be split into two populations: an older group of six grains with a weighted mean  $^{206}\text{Pb}/^{238}\text{U}$  age of  $264 \pm 7$  Ma ( $\chi^2$  value 0.21) and a younger group of six grains with a weighted mean  $^{206}\text{Pb}/^{238}\text{U}$  age of  $248 \pm 7$  Ma ( $\chi^2$  value 0.65). Zircons in the older group show strong oscillatory zoning of igneous origin and the age of  $264 \pm 7$  Ma is identical to other Permian granitoids previously

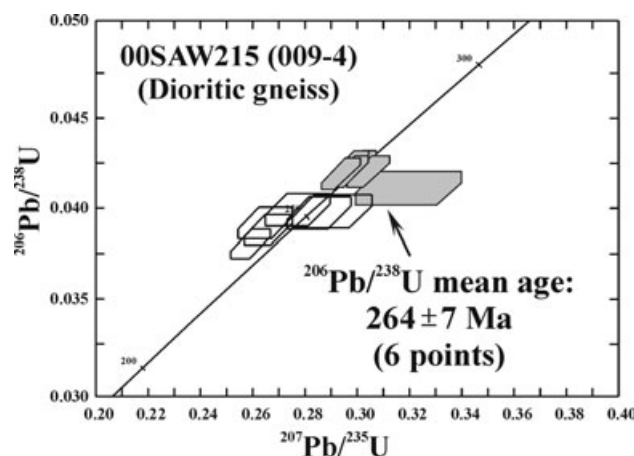


**Fig. 2** Concordia diagram showing sensitive high mass-resolution ion microprobe U-Pb zircon data for the dioritic gneiss sample 00SAW215 (009-4) in the Heilongjiang complex near Luobei. The grains with older ages (shaded) form a distinct group and show clear oscillatory zoning. Their age is interpreted as the emplacement age.

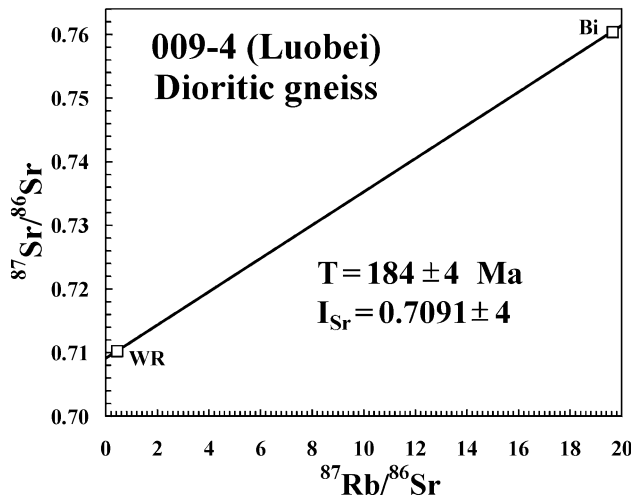


**Fig. 3** Biotite (Bi)-whole-rock (WR) Rb-Sr isochron for the dioritic gneiss sample 009-4 from the Heilongjiang complex near Luobei.

analyzed from the southern part of the Jiamusi Massif ( $264 \pm 11$  Ma) by Wilde *et al.* (1997). This is interpreted as the best estimate of the time of emplacement. The younger zircons show significantly lower amounts of U, Th and total Pb and most likely reflect recrystallization at, or later than,  $\sim 250$  Ma.

To constrain the metamorphic and deformation age of this rock, biotite from sample 0009-4 was selected for Rb-Sr analysis. The whole-rock and biotite Rb-Sr isochron yields an age of  $184 \pm 4$  Ma (Fig. 3). Because the above was only a two-point isochron, sample 0009-4 was also selected for biotite Ar-Ar laser dating. The results are plotted graphically in Figure 4. The apparent ages vary widely in the range of 174.2–197.6 Ma with a weighted mean age of  $184.9 \pm 3.5$  Ma (Fig. 4a). When they are plotted on the isochron diagram (Fig. 4b), the age is  $190.0 \pm 4.8$  Ma, identical to the weighted age within error. These ages are also identical to that of the Rb-Sr isochron, thus confirming the validity of the two-point isochron.

#### YILAN AREA

Sample 98105 was collected from Yilan and is intensely deformed two-mica schist composed of sillimanite, garnet, phengite, biotite, quartz and albite, with minor graphite. Sample 98118 was collected from Huanan, approximately 70 km east of Yilan, and has the same mineral assemblage as sample 98105, although the biotite content is a little higher. Sample 98117 is a muscovite-albite schist collected from Tuanshanzi near Yilan. It is fine-grained and composed of quartz, albite and

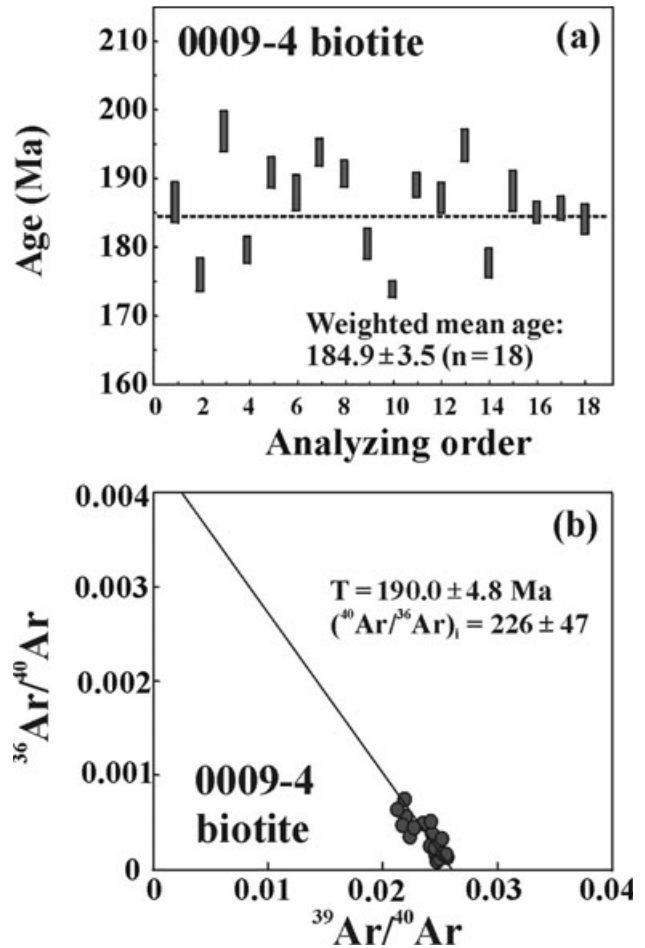


**Fig. 4** Biotite Ar-Ar ages of the dioritic gneiss sample 009-4 from the Heilongjiang complex near Luobei. (a) Weighted mean ages of the 18 grains of biotite analyzed by laser fusion. (b) Inverse isochron plotting of the above analyzed biotite grains.

phengite, with crossite present within albite porphyroblasts. The Ar-Ar data for these three samples are shown in Figure 5. All the phengites show flat age spectra and yield plateau ages of  $173.6 \pm 0.5$  Ma for sample 98105,  $175.3 \pm 0.4$  Ma for sample 98117 and  $174.8 \pm 0.5$  Ma for sample 98118 (Fig. 5). These plateau ages are perfectly consistent with each other. However, the K-Ar isotopic systematics of the biotite from sample 98105 are extremely disturbed, showing much younger apparent ages in the range of 48.8–73.9 Ma, with a total gas age of  $60.2 \pm 3.5$  Ma. This is difficult to explain, because the closure temperature of biotite is similar to that of white mica, which gives a consistent age of  $173.6 \pm 0.5$  Ma in this rock.

#### MUDANJIANG AREA

Sample FW02-182, collected from Mudanjiang, is a fine-grained two-mica schist with the mineral

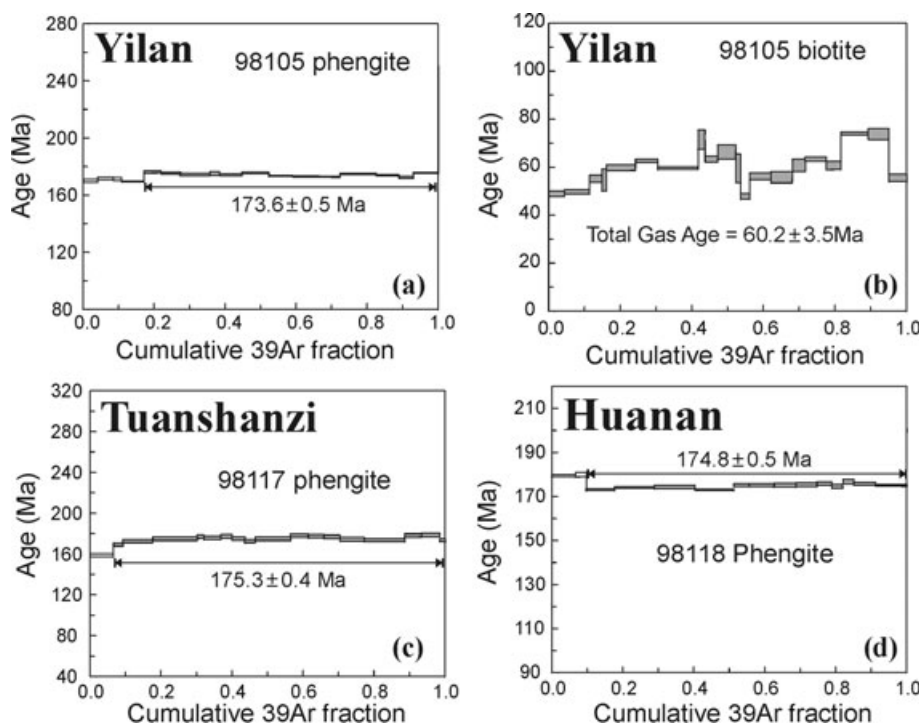


**Fig. 5** Ar–Ar ages of the two-mica schists from the Heilongjiang complex at Yilan and surrounding areas. All analyses were conducted by laser step heating method.

assemblage of quartz, plagioclase, potash feldspar, muscovite and biotite. Detrital zircons were selected for LA-ICPMS U–Pb analyses to constrain the maximum possible deposition age. The zircons are characterized by round shape and internal zoning, indicating their origin by weathering of igneous rocks. For the 19 analyses, one grain has a  $^{206}\text{Pb}/^{238}\text{U}$  age of  $321 \pm 1$  Ma; the remaining 18 analyses cluster into two groups with  $^{206}\text{Pb}/^{238}\text{U}$  weighted mean ages of  $279 \pm 3$  and  $251 \pm 1$  Ma, respectively (Fig. 6). These ages are similar to those of Permian granites in the Jiamusi block (Wu *et al.* 2001a). Although we tried to obtain the Ar–Ar and Rb–Sr isotopic ages of micas from this rock, the small size of the micas meant they were unsuitable for analysis.

## DISCUSSION

### TIMING OF METAMORPHISM IN THE HEILONGJIANG COMPLEX

Several geochronologic methods have been applied in an attempt to constrain the age of the Heilongjiang complex and its time of metamorphism. Using zircon U–Pb, whole-rock Sm–Nd and Rb–Sr techniques, it was previously concluded that the Heilongjiang complex was formed during the Archean to Mesoproterozoic (Cao *et al.* 1992; HBGMR 1993), and underwent blueschist to

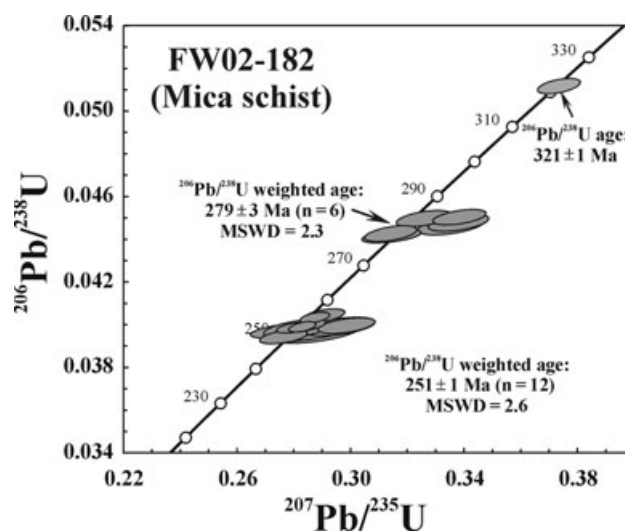


**Fig. 6** (U) Pb concordian diagram of detrital zircons from mica schist sample FW02-182 from the Heilongjiang complex near Mudanjiang. For explanation see text.

greenschist facies metamorphism during the early Paleozoic. However, all the reported zircon and whole-rock isochron ages have unrealistic errors, and no mineral that grew specifically during the metamorphism was dated. Zhang (1992) reported a whole-rock  $^{40}\text{Ar}/^{39}\text{Ar}$  age of  $645 \pm 32$  Ma for a blueschist and a plateau age of  $600 \pm 12$  Ma for glaucophane from Yilan, but it is hard to evaluate these data because no analytical data and procedures were presented. The discovery of Ordovician

Chitinozoans (? *Pseudodesmochina* sp., ? *Jenkinochititan* sp., *Laeosphaeridia*, *Cychochititan* sp., *Conochitina* sp.) from chert suggested that at least part of the Heilongjiang complex was Paleozoic in age (Sengör & Natal'in 1996; Li *et al.* 1999). Furthermore, although Ye and Zhang (1994) obtained a  $^{40}\text{Ar}/^{39}\text{Ar}$  plateau age of  $154.7 \pm 0.7$  Ma for crossite from a glaucophane-schist at Mudanjiang, they considered that the age reflected a later thermal event related to strike-slip movement along the Dunhua-Mishan Fault. The metamorphic age of the Heilongjiang complex thus remained unclear until the present study.

As stated above, the Heilongjiang complex is mainly composed of ophiolitic rocks with some shelf-type sediments and igneous rocks. Previous research indicated that most components have undergone blueschist facies metamorphism at  $\sim 350\text{--}450^\circ\text{C}$ , with a pressure of  $\sim 5\text{--}8$  kb (Yan *et al.* 1989; Cao *et al.* 1992; Li *et al.* 1999). This suggested that mica Rb–Sr and  $^{40}\text{Ar}/^{39}\text{Ar}$  methods could be used to constrain the time of metamorphism, because phengite is generally considered to have a Rb–Sr and Ar–Ar closure temperature in the range of  $350\text{--}400^\circ\text{C}$  or slightly above  $400^\circ\text{C}$  (Hames & Bowring 1994; Kirschner *et al.* 1996; Di Vincenzo *et al.* 2001).

In the Luobei area, the metamorphosed and deformed porphyritic dioritic gneiss has a U–Pb zircon intrusive age of  $264 \pm 7$  Ma (Fig. 2). The youngest detrital zircons in the mica schist from Mudanjiang have an age of  $251 \pm 1$  Ma (Fig. 6), indicating that the metamorphism must have been younger than Late Permian. Furthermore, biotite from the dioritic gneiss yields a Rb–Sr mineral isochron age of  $184 \pm 4$  Ma (Fig. 3), which is identical with the  $^{40}\text{Ar}/^{39}\text{Ar}$  age (Fig. 4). In the Yilan area (including Tuanshanzi and Huanan), three samples of mica schist gave phengite  $^{40}\text{Ar}/^{39}\text{Ar}$  ages of  $173.6 \pm 0.5$  Ma,  $175.3 \pm 0.4$  Ma and  $174.8 \pm 0.5$  Ma, just slightly younger than the ages obtained from Luobei. This general agreement of Rb–Sr and Ar–Ar ages from samples in the Luobei and Yilan areas is interpreted to mean that metamorphism of the Heilongjiang complex took place at the same time in all areas.

This is consistent with the work of Li *et al.* (1999) in the Mudanjiang area, where two muscovite samples from a mica schist gave  $^{40}\text{Ar}/^{39}\text{Ar}$  ages of  $175.3 \pm 0.9$  Ma and  $166 \pm 1.2$  Ma, and a hornblende from an amphibolite gave an age of  $167.1 \pm 1.5$  Ma.

The Heilongjiang complex in all three outcrop areas thus exhibits a similar metamorphic age. It

is concluded that blueschist- to greenschist-facies metamorphism throughout the Heilongjiang complex took place in the Jurassic.

#### THE JIAMUSI MASSIF AS AN ACCRETED TERRANE: GEOCHRONOLOGIC CONSTRAINTS

The Jiamusi Massif is an important tectonic unit, being one of only four fragments located in the CAOB or Altaid Collage (Sengör *et al.* 1993) in northeastern China. It is believed to extend northward into the Bureya Massif and eastward into the Khanka Massif in Far East Russia (Natal'in & Borukayev 1991; Cao *et al.* 1992).

According to the regional geological survey of the HBGMR (1993) and our investigations, the Jiamusi Massif is composed of the Mashan and Heilongjiang complexes, and deformed and undeformed granitoids. Few investigations have been undertaken on the deformed granites, which form tectonic sheets separating and dismembering the khondalitic units of the Mashan complex, or on the plutons of variably deformed granitoids that are commonly associated with these metasedimentary rocks. These granitoids have been considered Archean–Paleoproterozoic in age on the most recent geological map of the area (Zhao *et al.* 1996), although no precise geochronologic work was undertaken. However, our recent SHRIMP U–Pb zircon analyses indicate that these granites were emplaced between 530 and 515 Ma (Wilde *et al.* 2003). A deformed pegmatite from Liu Mao, which intrudes the Mashan complex and contains oscillatory-zoned igneous zircons, has a weighted mean  $^{206}\text{Pb}/^{238}\text{U}$  age of  $530 \pm 11$  Ma, interpreted to be the age of crystallization of the pegmatite. A deformed granitoid from Sandaogou near Jixi contains zircons with well-defined oscillatory zoning that define a weighted mean  $^{206}\text{Pb}/^{238}\text{U}$  age of  $523 \pm 8$  Ma, taken to be the age of the granite protolith. Also, a weakly deformed porphyritic granite from near Jiamusi, which contains oscillatory-zoned zircon, has a weighted mean  $^{206}\text{Pb}/^{238}\text{U}$  Ma crystallization age of  $515 \pm 8$  Ma. Several zircon crystals from both granite samples show evidence of recrystallization at  $505 \pm 4$  Ma and  $497 \pm 5$  Ma in the Sandaogou and Jiamusi samples, respectively, and this is attributed to the granulite facies metamorphic event that affected the southern outcrop area of the Mashan complex.

The khondalitic metasedimentary rocks of the Mashan complex include graphite and sillimanite-bearing schists and gneisses and diopside and olivine-bearing marbles, which have been meta-

morphosed to amphibolite/granulite facies. Although the deposition age of these rocks was considered as Archean (HBGMR 1993), our zircon U–Pb and Nd isotopic results do not support this interpretation (Wilde *et al.* 1997, 2000; B-M. Jahn, unpubl. data, 2005). A sillimanite gneiss from Sandaogou contains a single population of metamorphic zircons with a  $^{206}\text{Pb}/^{238}\text{U}$  age of  $496 \pm 8$  Ma. Sillimanite gneiss from Xi Mashan, approximately 3 km west of Mashan, has a  $^{206}\text{Pb}/^{238}\text{U}$  metamorphic zircon age of  $\sim 500$  Ma, but also includes several populations of detrital zircon grains that extend back to *ca* 1800 Ma. A garnetiferous granite from Xi Mashan has a  $^{206}\text{Pb}/^{238}\text{U}$  igneous zircon age of  $507 \pm 12$  Ma. It contains an enclave of garnet paragneiss and this has a metamorphic zircon age of *ca* 500 Ma. These data establish that the khondalites of the Mashan complex record an early Paleozoic Pan-African metamorphic event. The older zircon populations in the sillimanite gneiss and garnet gneiss enclave from Xi Mashan indicate derivation from both Paleo- and Mesoproterozoic sources.

Permian undeformed granites are also widely distributed in the Jiamusi Massif. They locally show magmatic foliation, but no signs of deformation or metamorphism. Previously, these granites were considered to have formed in the Neoproterozoic, because Rb–Sr whole-rock isochron age of  $626 \pm 64$  Ma was obtained (Li & Zhao 1987; HBGMR 1993). However, if we recalculate the original data using ISOPLOT (Ludwig 1999) with input errors of 2% for  $^{87}\text{Rb}/^{86}\text{Sr}$  and 0.05% for  $^{87}\text{Sr}/^{86}\text{Sr}$ ; this age is an ‘errorchron’ which is geologically meaningless. Song *et al.* (1994) analyzed zircons using the evaporation method and reported ages in the range of 312–250 Ma, indicating these granites might have been emplaced during the Paleozoic period. However, this dating method, yielding  $^{207}\text{Pb}/^{206}\text{Pb}$  ages, is not ideal for young complex zircons, because the  $^{206}\text{Pb}/^{238}\text{U}$  age is more precise for Phanerozoic zircons (Compston *et al.* 1992). Our recent zircon SHRIMP U–Pb dating of four plutons at Chaihe, Chushan and Qingshan, north of Mudanjiang, and at Shichang near Jixi, suggests that they were emplaced in the Late Paleozoic between 270 and 254 Ma (Wu *et al.* 2000, 2001a). Inherited zircon grains or cores in some zircons grains support the view that they resulted from partial melting of basement rocks in the Jiamusi Massif, but their geodynamic implications are unclear (Wu *et al.* 2001a).

From the above review of the available geochronologic data, the early tectonic evolution of the

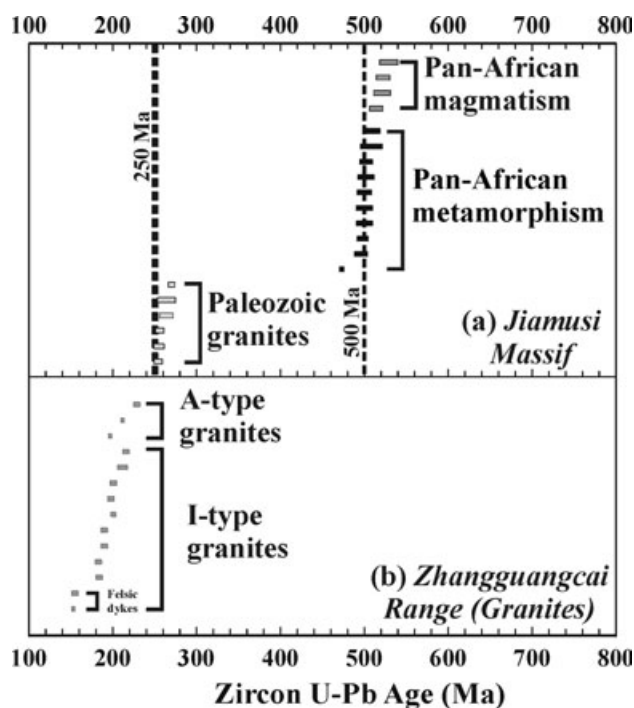


**Fig. 7** Compilation of zircon U–Pb ages for the Jiamusi Massif (a) and the Zhangguangcai Range (b) (Data sources: Wilde *et al.* 1997, 2000, 2003; Wu *et al.* 2000, 2001a, 2002, 2003).

Jiamusi Massif can be summarized as follows (Fig. 7a). During the Proterozoic, a khondalite sequence was deposited at an unknown continental margin. This area was then affected by magmatism between 530 and 515 Ma, followed by granulite/amphibolite facies metamorphism at *ca* 500 Ma. Another stage of granitic magmatism took place in the Permian at 270–254 Ma. The Jiamusi Massif thus experienced both Pan-African and Late Paleozoic events, neither of which is identified in the surrounding Zhangguangcai Range (Fig. 7b).

However, the paleogeographic location of the Jiamusi Massif throughout this history is unclear. In the CAOB, the unique Pan-African event developed in the Mashan complex is rarely documented in other locations. Salnikova *et al.* (1998) have reported ages of  $488 \pm 0.5$  and  $478 \pm 2$  Ma for the emplacement of pyroxene-bearing trondhjemite and subsequent granulite facies metamorphism of the Sludyanskiy complex in the southwestern Baikal region, at the southern margin of the Siberian Craton. This was followed by post-tectonic emplacement of quartz syenite at  $471 \pm 2$  Ma. On the basis of these data and other geological constraints, Salnikova *et al.* (1998) distinguish a high-grade Paleozoic metamorphic terrain that extends for more than 1000 km along the southern margin of the Siberian Craton, which was subsequently

verified by dating the Tuva-Mongolian Massif in western Mongolia, where Neoproterozoic (*ca* 800–900 Ma) and Early Paleozoic (*ca* 500 Ma) events have been identified (Kuzmichev *et al.* 2001; Salnikova *et al.* 2001). In contrast, Wilde *et al.* (1999, 2000, 2003) proposed, in view of the Pan-African ages, that the Jiamusi Massif might have been part of Gondwana, because *ca* 500 Ma metamorphic events and *ca* 530 Ma granitic intrusions are found in Prydz Bay, East Antarctica (Kinny *et al.* 1993; Hensen & Zhou 1995) and in South Australia (Flottmann *et al.* 1994; Sandiford *et al.* 1995; Turner & Foden 1996; Foden *et al.* 1999); a recent summary by Veevers (2004) supports this speculation. Therefore, one possible scenario is that the Jiamusi Massif was located at the edge of the Gondwana supercontinent during the early Paleozoic and then drifted northward, eventually amalgamating with the Asian continent in the Jurassic. However, the exact significance of the Heilongjiang complex to this needs to be examined in more detail below.

#### JURASSIC ACTIVE CONTINENTAL MARGIN IN EASTERN ASIA

In the CAOBS, final suturing between the Siberian and North China cratons took place between the Late Permian and Early Triassic (Zonenshain *et al.* 1985; Dobretsov *et al.* 1990, 1995; Sengör *et al.* 1993; Sengör & Natal'in 1996; Xiao *et al.* 2003), which makes the Jurassic collision of the Jiamusi Massif an enigma. However, Jurassic accretionary terranes are widely distributed along the eastern Asian continental margin (Natal'in & Borukayev 1991; Natal'in 1993; Sengör & Natal'in 1996).

In northeastern Russia, the Mesozoic Verkhoyansk-Kolyma Orogenic Belt developed between the Siberian and North American cratons (Parfenov 1991; Oxman *et al.* 1995; Layer *et al.* 2001; Oxman 2003). Although the relationship between the Kolyma-Omolon block and Siberian Craton is controversial (Popeko *et al.* 1993; Dobretsov *et al.* 1995; Gordienko 1996; Stone *et al.* 2003), structural analysis supports the view that suturing between them took place in the Jurassic, with collision before the Bathonian-Callovia (*ca* 168–161 Ma) (Parfenov 1991). Ar–Ar dating of greenschist facies metamorphic muscovite from the Chersky Range ophiolite indicates that suturing took place at *ca* 174–170 Ma (Oxman *et al.* 1995), which is also verified by the age of the plutonic rocks (Layer *et al.* 2001).

Farther south in Far East Russia, no Mesozoic accretionary complex has been identified to the west of the Bureya Massif (Natal'in 1991, 1993). However, the Triassic–Jurassic Badzhal unit, consisting mainly of Paleozoic limestone olistoliths in a clastic matrix, Permian and Triassic chert lenses, Late Triassic through to Late Jurassic turbidites, chert and siliceous shale and small lenses of mafic volcanic rocks (Natal'in 1991, 1993; Nokleberg *et al.* 2001), is interpreted as a Triassic–Jurassic accretionary complex composed of tectonically intermixed oceanic and continental-slope deposits (Natal'in 1991, 1993; Nokleberg *et al.* 2001). It was traditionally thought that this accretionary terrane is located to the east of the Bureya Massif. Our field investigations indicate that the south Malokhingian block in this massif is the possible northern continuation of the Jiamusi Massif. However, the northern Turan block is mostly occupied by various granites, very similar to the Zhangguangcai Ranges farther south in China. Therefore, it is suggested that the Badzhal unit could be considered as the accretionary terrane between the Malokhingian and Turan blocks, and therefore related to circum-Pacific orogenesis (Sengör & Natal'in 1996). A review of the published reports indicates that the Badzhal unit is most likely the northern extension of the Heilongjiang complex, although more work is needed to verify this conclusion. South of this area, Jurassic accretionary complexes at Nadanhada in northeastern China and Khabarovsk in Far East Russia have been identified (Kojima 1989; Natal'in & Zyabrev 1989; Natal'in 1991, 1993; Parfenov *et al.* 1993; Popova *et al.* 1999; Zyabrev & Matsuoka 1999; Khanchuk 2001), where Cretaceous accretionary complexes are also developed to the east (Natal'in & Zyabrev 1989; Natal'in 1991, 1993; Khanchuk 2001).

In the Japanese islands, a Jurassic accretionary terrane occurs as a large-scale nappe that is tectonically sandwiched between overlying pre-Jurassic and underlying post-Jurassic sequences (Isozaki 1997; Maruyama 1997; Takahashi 1999). Accretion lasted over 80 Ma, from the latest Triassic to the earliest Cretaceous (but mainly took place in the Middle Jurassic; Isozaki 1997; Taira 2001). It is suggested that this Jurassic accretionary complex extends for approximately 6000 km from the Koryak region in Russia to North Palawan in the Philippines (Isozaki *et al.* 1987; Kojima 1989; Faure & Natal'in 1992; Isozaki 1997; Zamoras & Matsuoka 2004).

From the above discussion, it is clear that Mesozoic accretionary terranes are widely distributed along the Asian continental margin. The Early Middle Jurassic accretionary complexes are mainly developed to the east of the Siberia Craton in north-eastern Russia and to the west of the Khanka-Jiamusi-Bureya block which shows an affinity to Gondwana. The Late Jurassic accretionary complexes are mainly exposed farther eastward and are overlapped by the Cretaceous complexes, which is similar to the situation in the Japanese Islands, indicating an eastward younging trend. It can therefore be concluded that the eastern Asian continental margin evolved in a subduction-related tectonic setting since at least the Early Jurassic.

Another line of supporting evidence to the above interpretation is the occurrence of Mesozoic arc-related magmatism in northeastern Russia and northeastern China. Geochronologic evidence presented by Miller *et al.* (2002) suggests that magmatism in northeastern Russia occurred in two stages: Late Triassic to Early Jurassic and Late Jurassic to Early Cretaceous with tectonic quiescence in between. In the northern Zhangguangcai Range of northeastern China, more than 90% of the voluminous I-type granites were emplaced between  $216 \pm 4$  and  $184 \pm 4$  Ma (Wu *et al.* 2000; Fig. 7b), which can be correlated to the first stage of magmatism in northeastern Russia. Accordingly, it is suggested that the Late Triassic to Early Jurassic magmatism in the Zhangguangcai Range

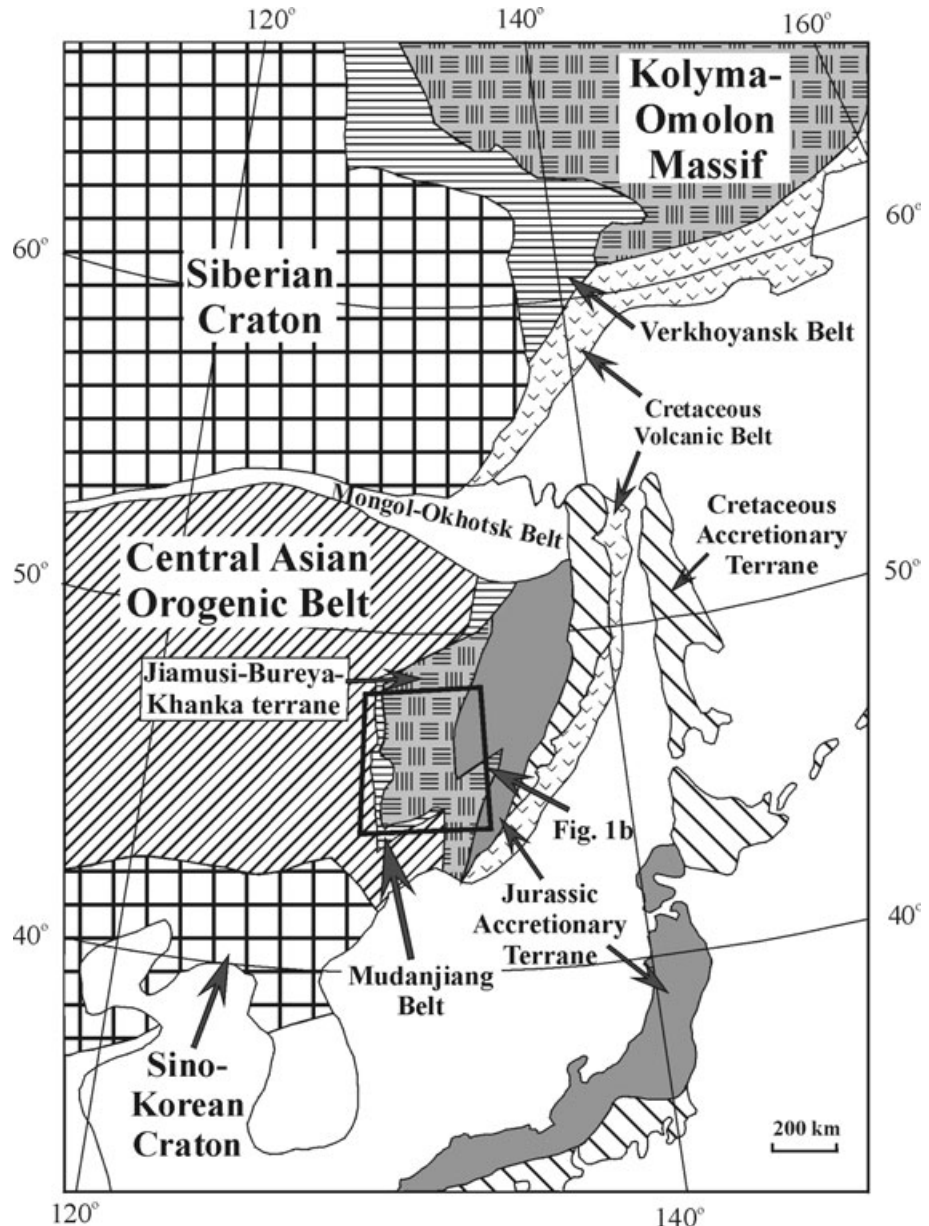


**Fig. 8** Mesozoic accretionary complexes along the northeastern Asian continental margin (based on map by Shao & Tang 1995). The box shows the position of studied area of Figure 1b.

is related to the suturing along the Mudanjiang Belt between the Jiamusi Massif and the evolving western continent (Fig. 8), forming part of the CAOB. This view is different from the conclusion of Sengör and Natal'in (1996) that the Great Xing'an Range farther to the west was an arc during the above subduction.

## CONCLUSIONS

From our study of the Heilongjiang complex in northeastern China, it can be concluded that:

1. The Heilongjiang complex is a tectonic mélange that includes granitic gneiss, marble, mafic-ultramafic rocks, blueschist, greenschist, quartzite and mica schist. The marble and granitic gneiss were probably derived from the neighboring Mashan complex, whereas the remainder are most likely constituents of ophiolite. These rocks are now tectonically interleaved and were deformed together;
2. SHRIMP U–Pb zircon analyses of the granitic gneiss show the protolith granite was emplaced at  $264 \pm 7$  Ma, coeval with the emplacement of Permian batholiths elsewhere in the Jiamusi Massif.  $^{40}\text{Ar}/^{39}\text{Ar}$  dating of biotite from the granitic gneiss and phengite from mica schists indicate that blueschist facies metamorphism occurred at *ca* 184–174 Ma in the Early Jurassic, not in the Early Paleozoic as previously thought. These new data strongly indicate that the Heilongjiang complex is an Early Jurassic accretionary complex;
3. The early components of the Jiamusi Massif probably form part of an exotic terrane from Gondwana that was affected by late Pan-African orogenesis, and which collided with the Asian continental margin during the Early Jurassic, as indicated by the blueschist facies metamorphism of the intervening Heilongjiang complex. Therefore, it is suggested that a continental margin existed at least since the Early Jurassic along the eastern Asian continental margin and was affected by Late Jurassic to Cretaceous subduction and accretionary processes. This belt extends from Far East Russia, through northeastern China and the Japanese Islands, resulting in the extensive development of Mesozoic plutonic-volcanic rocks along the eastern Asian continental margin, as in the Zhanggaungcai Range.

## ACKNOWLEDGEMENTS

We are most grateful to the laboratory staff of the Isotopic Laboratory, Institute of Geology and Geophysics, Chinese Academy of Sciences in Beijing, and to Dr X. M. Liu, Department of Geology, North-west University in Xi'an for help with collecting the ICP-MS data. Dr Matthew Grant kindly assisted with collection of the SHRIMP data and the SHRIMP II facility is operated by the Perth Consortium, comprising Curtin University of Technology, the University of Western Australia and the Geological Survey of Western Australia. We are grateful for constructive reviews by Drs Y. Isozaki, I. Kaneoka, B. A. Natal'in and S. Wallis. This work was supported by the National Natural Science Foundation of China (NSFC grants 40325006, 40502010 and 40421202) and Key Laboratory of Continental Dynamics at North-west University.

## REFERENCES

- ANDERSEN T. 2002. Correction of common lead in U–Pb analyses that do not report  $^{204}\text{Pb}$ . *Chemical Geology* **192**, 59–79.
- CAO X., DANG Z. X., ZHANG X. Z., JIANG J. S. & WANG H. D. 1992. *The Composite Jiamusi Terrane*. Jilin Publishing House of Science and Technology, Changchun (in Chinese with English and Russian abstracts).
- CHEN P. R., HUA R. M., ZHANG B. T., LU J. J. & FAN C. F. 2002. Early Yanshanian post-orogenic granitoids in the Nanling region. *Science in China (D)* **45**, 755–68.
- CHOUGH S. K., KWON S. T., REE J. H. & CHOI D. K. 2000. Tectonic and sedimentary evolution of the Korean peninsula: A review and new view. *Earth Science Review* **52**, 175–235.
- COMPSTON W., WILLIAMS I. S., KIRSCHVINK J. L., ZHANG Z. & MA G. 1992. Zircon U–Pb ages for the Early Cambrian time-scale. *Journal of Geological Society London* **149**, 171–84.
- DENG J. F., MO X. X., ZHAO H. L., WU Z. X., LUO Z. H. & SU S. G. 2004. A new model for the dynamic evolution of Chinese lithosphere: 'continental roots-plume tectonics'. *Earth Science Review* **65**, 223–75.
- DI VINCENZO G., GHIRIBELLI B., GIORGETTI G. & PALMERI R. 2001. Evidence of a close link between petrology and isotope records: Constraints from SEM, EMP, TEM and in situ  $^{40}\text{Ar}$ – $^{39}\text{Ar}$  laser analyses on multiple generations of white micas (Lanternman Range, Antarctica). *Earth and Planetary Science Letters* **192**, 389–405.

- DOBRETISOV N. L., DOOK V. L. & KITSUL V. I. 1990. Geotectonic evolution of the Siberian platform during the Precambrian and comparison with the lower Precambrian complexes of eastern Asia. *Journal of Southeastern Asian Earth Sciences* **4**, 259–66.
- DOBRETISOV N. L., BERZIN N. A. & BUSLOV M. 1995. Opening and tectonic evolution of the Paleo-Asian Ocean. *International Geology Review* **37**, 335–60.
- FAN W. M., GUO F., WANG Y. J. & LIN G. 2003. Late Mesozoic calc-alkaline volcanism of post-orogenic extension in the northern Da Hinggan Mountains, Northeastern China. *Journal of Volcanology and Geothermal Research* **121**, 115–35.
- FAURE M. & NATAL'IN B. 1992. The geodynamic evolution of the eastern Eurasian margin in Mesozoic times. *Tectonophysics* **208**, 397–411.
- FAURE M., NATAL'IN B. A., MONIE P., VRUBLEVSKY A. A., BORUKAIEV CH. & PRIKHODKO V. 1995. Tectonic evolution of the Anuy metamorphic rocks (Sikhote Alin, Russia) and their place in the Mesozoic geodynamic framework of East Asia. *Tectonophysics* **241**, 279–301.
- FLOTTMANN T., JAMES P., ROGERS J. & JOHNSON T. 1994. Early Palaeozoic foreland thrusting and basin reactivation at the Palaeo-Pacific margin of the southeastern Australian Precambrian Craton: A reappraisal of the structural evolution of the southern Adelaide Fold-thrust Belt. *Tectonophysics* **234**, 95–116.
- FODEN J., SANDIFORD M., DOUGHERTY-PAGE J. & WILLIAMS I. 1999. Geochemistry and geochronology of the Rathjen Gneiss: Implications for the early tectonic evolution of the Delamerian Orogen. *Australian Journal of Earth Sciences* **46**, 377–89.
- FU J. M., MA C. Q., XIE C. F., ZHANG Y. M. & PENG S. B. 2004. The determination of the formation ages of the Xishan volcanic-intrusive complex in southern Hunan province. *Acta Geoscientica Sinica* **25**, 303–8 (in Chinese with English abstract).
- GE W. C., WU F. Y., ZHOU C. Y. & ABDEL RAHMAN A. A. 2005a. Emplacement age of the Tahe granite and its constraints on the tectonic nature of the Eguna block in the northern part of the Great Xing'an Range. *Chinese Science Bulletin* **50**, 2097–105.
- GE W. C., WU F. Y., ZHOU C. Y. & ZHANG J. H. 2005b. Zircon U–Pb ages and its significance of the Mesozoic granites in the Wulanhaote region, central Da Hinggan Mountain. *Acta Petrologica Sinica* **21**, 749–62.
- GILDER S. A., GILL J., COE R. S. *et al.* 1996. Isotopic and paleomagnetic constraints on the Mesozoic tectonic evolution of south China. *Journal of Geophysical Research* **101**, 16137–54.
- GORDIENKO I. V. 1996. Correlation of Pre-Jurassic sections of ancient continents and microcontinents in East Asia. *Journal of Southeastern Asian Earth Sciences* **13**, 215–21.
- HAMES W. E. & BOWRING S. A. 1994. An empirical evaluation of the argon diffusion geometry in muscovite. *Earth and Planetary Science Letters* **124**, 161–7.
- HBGMR (HEILONGJIANG BUREAU OF GEOLOGY AND MINERAL RESOURCES). 1993. *Regional Geology of Heilongjiang Province*. Geological Publishing House, Beijing (in Chinese with English abstract).
- HENSEN B. J. & ZHOU B. 1995. A Pan-African granulite facies metamorphic episode in Prydz Bay, Antarctica: Evidence from Sm–Nd garnet dating. *Australian Journal of Earth Sciences* **42**, 249–58.
- ISOZAKI Y. 1997. Jurassic accretion tectonics of Japan. *Island Arc* **6**, 25–51.
- ISOZAKI Y., AMISCARAY E. A. & RILLON A. 1987. Permian, Triassic and Jurassic bedded radiolarian cherts in North Palawan block, Philippines: Evidence of late Mesozoic subduction-accretion. *Journal of Geological Society of Philippines* **31**, 79–93.
- JACKSON S. E., PEARSON N. J., GRIFFIN W. L. & BELOUSOVA E. A. 2004. The application of laser ablation-inductively coupled plasma-mass spectrometry (LA-ICP-MS) to in situ U–Pb zircon geochronology. *Chemical Geology* **211**, 47–69.
- JAHN B. M. 2004. The Central Asian Orogenic Belt and growth of the continental crust in the Phanerozoic. In Malpas J. Fletcher C. J. N. Ali J. R. & Aitchison J. C. (eds). *Aspects of the Tectonic Evolution of China*. 226, 73–100. Geological Society of London, Special Publication.
- JAHN B. M., WU F. Y. & CHEN B. 2000. Massive granitoid generation in central Asia: Nd isotopic evidence and implication for continental growth in the Phanerozoic. *Episodes* **23**, 82–92.
- KHANCHUK A. I. 2001. Pre-Neogene tectonics of the Sea-of-Japan region: A view from Russian side. *Earth Science (Chikyū Kagaku)* **55**, 275–91.
- KINNY P. D., BLACK L. P. & SHERATON J. W. 1993. Zircon ages and the distribution of Archaean and Proterozoic rocks in the Rauer Islands. *Antarctic Sciences* **5**, 193–206.
- KIRSCHNER D. L., COSCA M. A., MASSON H. & HUNZIKER J. C. 1996. Staircase  $^{40}\text{Ar}/^{39}\text{Ar}$  spectra of fine-grained white mica: Timing and duration of deformation and empirical constraints on argon diffusion. *Geology* **24**, 747–50.
- KOJIMA S. 1989. Mesozoic terrane accretion in northeast China, Sikhote-Alin and Japan regions. *Palaeos* **69**, 213–32.
- KUZMICHEV A. B., BIBIKOVA E. V. & ZHURAVLEV D. Z. 2001. Neoproterozoic (~800 Ma) orogeny in the Tuva-Mongolia Massif (Siberia): Island arc–continent collision at the northeast Rodinia margin. *Precambrian Research* **110**, 109–26.
- LAYER P. W., NEWBERRY R., FUJITA K., PARFENOV L., TRUNILINA V. & BAKHAREV A. 2001. Tectonic setting of the tectonic belts of Yakutia, northeast Russia, based on  $^{40}\text{Ar}/^{39}\text{Ar}$  geochronology and trace element geochemistry. *Geology* **29**, 167–70.

- LI J. Y. 2006. Permian geodynamic setting of Northeast China and adjacent regions: Closure of the Paleo-Asian Ocean and subduction of the Paleo-Pacific Plate. *Journal of Asian Earth Sciences* **26**, 207–24.
- LI J. Y., NIU B. G., SONG B., XU W. X., ZHANG Y. H. & ZHAO Z. R. 1999. *Crustal Formation and Evolution of Northern Changbai Mountains, Northeast China*. Geological Publishing House, Beijing (in Chinese with English abstract).
- LI X. H., CHEN Z. G., LIU D. Y. & LI W. X. 2003. Jurassic gabbro-granite-syenite suites from southern Jiangxi Province, SE China: Age, origin, and tectonic significance. *International Geology Review* **45**, 898–921.
- LI Z. T. & ZHAO C. J. 1987. On the characteristics and origin of Singkainian granodiorite body in Chushan Mountain, east Heilongjiang province (in Chinese with English abstract). *Acta Petrologica Sinica* **1**, 3–16.
- LO C. H., CHUNG S. L., LEE T. Y. & WU G. Y. 2002. Age of the Emeishan flood magmatism and relations to Permian–Triassic boundary events. *Earth and Planetary Science Letters* **198**, 449–58.
- LUDWIG K. R. 1999. *Isoplot/Ex (v. 2.06) – A Geochronological Toolkit for Microsoft Excel*. Berkeley Geochronology Center, Berkeley. Special Publisher No. 1a, 49 pp.
- MARUYAMA S. 1997. Pacific-type orogeny revisited: Miyashiro-type orogeny proposed. *Island Arc* **6**, 91–120.
- MIAO L. C., FAN W. M., ZHANG. F. Q. *et al.* 2004. SHRIMP zircon geochronology of the Xinkailing-Kele complex in the northwestern Lesser Xing'an Range, and its geological implications. *Chinese Science Bulletin* **49**, 201–9.
- MILLER E. L., GEIMAN M., PARFENOV L. & HOURIGAN J. 2002. Tectonic settings of Mesozoic magmatism: A comparison between northeastern Russia and the North American Cordillera. In Miller E. L., Grantz A. & Klempner S. L. (eds). *Tectonic Evolution of the Bering Shelf-Chukchi Sea-Arctic Margin and Adjacent Landmasses*. 360, 313–32. Geological Society of America Special Paper.
- NATAL'IN B. A. 1991. Mesozoic accretion and collision tectonics of southern USSR Far East. *Pacific Geology* **10**, 3–23.
- NATAL'IN B. A. 1993. History and modes of Mesozoic accretion in southeastern Russia. *Island Arc* **2**, 15–34.
- NATAL'IN B. A. & BORUKAYEV C. B. 1991. Mesozoic sutures in the southern Far East of USSR. *Geotectonics* **25**, 64–74.
- NATAL'IN B. A. & ZYABREV S. V. 1989. Structural geology of Mesozoic rocks of the Amur River Valley. Dal'nevost. Otd. Akad. Nauk SSSR, Field Trip Guidebook, Khabarovsk, 47pp.
- NELSON D. R. 1997. *Compilation of Geochronology Data, 1996*. Geological Survey of Western Australia, Perth. Geological Survey of Western Australia Record 1997/2, 189 pp.
- NOKLEBERG W. J., PARFENOV L. M., MONGER J. W. H. *et al.* 2001. Phanerozoic tectonic evolution of the Circum-North Pacific. *U.S. Geological Survey Professional Paper* **1626**, 122p.
- OXMAN V. S. 2003. Tectonic evolution of the Mesozoic Verkhoyansk–Kolyma belt (NE Asia). *Tectonophysics* **365**, 45–76.
- OXMAN V. S., PARFENOV L. M., PROKOPIEV A. V. *et al.* 1995. The Chersky Range ophiolite belt, northeast Russia. *Journal of Geology* **103**, 539–56.
- PARFENOV L. M. 1991. Tectonics of the Verkhoyansk–Kolyma Mesozoides in the context of plate tectonics. *Tectonophysics* **199**, 319–42.
- PARFENOV L. M., NATAPOV L. M., SOKOLOV S. D. & TSUKANOV N. V. 1993. Terranes analysis and accretion in northeast Asia. *Island Arc* **2**, 35–54.
- PIDGEON R. T., FURFARO D., KENNEDY A. K., NEMCHIN A. A., VAN BRONSWIJK W. & TODT W. A. 1994. Calibration of zircon standards for the Curtin SHRIMP II. *Abstract of Eighth International Conference on Geochronology, Cosmochronology and Isotope Geology*, 251.
- POPEKO L. I., NATAL'IN B. A., BELYAYEVA G. V., KOTLYAR G. V. & SHISHKINA G. R. 1993. Paleobiogeographic zoning of Paleozoic and geodynamics of southern Russian Far East. *Pacific Geology* **12**, 19–30.
- POPOVA I. M., BAUMGARTNER P. O., FILIPPOV A. V. & KHANCHUK A. I. 1999. Jurassic and early cretaceous Radiolaria of the lower Amurian terrane: Khabarovsk region, far east of Russia. *Island Arc* **8**, 491–522.
- RENNE P. R., SWISHER C. C., DEINO A. L., KARNER D. B., OWENS T. L. & DEPAOLO D. J. 1998. Intercalibration of standards, absolute ages and uncertainties in  $^{40}\text{Ar}/^{39}\text{Ar}$  dating. *Chemical Geology* **145**, 117–52.
- SAGONG H., KWON S. T. & REE J. H. 2005. Mesozoic episodic magmatism in south Korea and its tectonic implication. *Tectonics* **24**, 2004TC001720.
- SALNIKOVA E. B., SERGEEV S. A., KOTOV A. B. *et al.* 1998. U-Pb zircon dating of granulite metamorphism in the Sludyanskiy Complex, eastern Siberia. *Gondwana Research* **1**, 195–205.
- SALNIKOVA E. B., KOZAKOV I. K., KOTOV A. B. *et al.* 2001. Age of Palaeozoic granites and metamorphism in the Tuvino-Mongolian Massif of the Central Asian Mobile Belt: Loss of a Precambrian microcontinent. *Precambrian Research* **110**, 143–64.
- SANDIFORD M., FRASER G., ARNOLD J., FODEN J. & FARROW T. 1995. Some causes and consequences of high-temperature, low-pressure metamorphism in the northern Flinders Ranges, South Australia. *Australian Journal of Earth Sciences* **42**, 233–40.
- SENGÖR A. M. C. & NATAL'IN B. A. 1996. Paleotectonics of Asia: Fragments of a synthesis. In Yin A. & Harrison M. (eds). *The Tectonic Evolution of Asia*, pp. 486–640. Cambridge University Press, Cambridge.

- SENGÖR A. M. C., NATAL'IN B. A. & BURTMAN V. S. 1993. Evolution of the Altaid tectonic collage and Palaeozoic crustal growth in Eurasia. *Nature* **364**, 299–307.
- SHAO J. A. & TANG K. D. 1995. *Terranes in Northeast China and Evolution of Northeast Asia Continental Margin*. Seismic Press, Beijing.
- SONG B., NIU B. G., LI J. Y. & XU W. X. 1994. Isotope geochronology of granitoids in Mudanjiang-Jixi area (in Chinese with English abstract). *Acta Petrologica et Mineralogica* **13**, 204–13.
- STONE D. B., MINYUK P. & KOLOSEV E. 2003. New paleomagnetic paleolatitudes for the Omulevka terrane of northeast Russia: A comparison with the Omolon terrane and the eastern Siberian platform. *Tectonophysics* **377**, 55–82.
- TAIRA A. 2001. Tectonic evolution of the Japanese island arc system. *Annual Review of Earth and Planetary Sciences* **29**, 109–34.
- TAKAHASHI M. 1983. Space-time distribution of late Mesozoic to early Cenozoic magmatism in east Asia and its tectonic implications. In Hashimoto M. & Uyeda S. (eds). *Accretion Tectonics in the Circum-Pacific Regions*. Terra Scientific Publishing Company, Tokyo, 69–88.
- TAKAHASHI O. 1999. Polyphase accretionary tectonics in the Jurassic to Cretaceous accretionary belts of Central Japan. *Island Arc* **8**, 349–58.
- TURNER S. P. & FODEN J. D. 1996. Magma mingling in late-Delamerian A-type granites at Mannum, South Australia. *Mineralogy and Petrology* **56**, 147–69.
- VEEVERS J. J. 2004. Gondwanaland from 650 to 500 Ma assembly through 320 Ma merger in Pangea to 185–100 Ma breakup: Supercontinental tectonics via stratigraphy and radiometric dating. *Earth Science Review* **68**, 1–132.
- WANG L. G., QIU Y. M., MCNAUGHTON N. J. *et al.* 1998. Constraints on crustal evolution and gold metallogeny in the northwestern Jiaodong Peninsula, China, from SHRIMP U-Pb zircon studies of granitoids. *Ore Geology Review* **13**, 275–91.
- WILDE S. A., DORSETT-BAIN H. L. & LIU J. L. 1997. The identification of a Late Pan-African granulite facies event in Northeastern China: SHRIMP U-Pb zircon dating of the Mashan Group at Liu Mao, Heilongjiang Province, China. *Proceedings of the 30th IGC: Precambrian Geology and Metamorphic Petrology, VSP International*. Science Publishers, Amsterdam. **17**, 59–74.
- WILDE S. A., DORSETT-BAIN H. L. & LENNON R. G. 1999. Geological setting and controls on the development of graphite, sillimanite and phosphate mineralisation within the Jiamusi Massif: An exotic fragment of Gondwanaland located in North-Eastern China? *Gondwana Research* **2**, 21–46.
- WILDE S. A., ZHANG X. Z. & WU F. Y. 2000. Extension of a newly-identified 500 Ma metamorphic terrain in Northeast China: Further U-Pb SHRIMP dating of the Mashan Complex, Heilongjiang Province, China. *Tectonophysics* **328**, 115–30.
- WILDE S. A., WU F. Y. & ZHANG X. Z. 2003. Late Pan-African magmatism in Northeastern China: SHRIMP U-Pb zircon evidence for igneous ages from the Mashan Complex. *Precambrian Research* **122**, 311–27.
- WILLIAMS I. S. 1998. U-Th-Pb geochronology by ion microprobe. In Mckibben M. A. Shanks W. C. III & Ridley W. I. (eds). *Applications of Microanalytical Techniques to Understanding Mineralizing Processes*, pp. 1–35. Society of Economic Geologists, Colorado. *Reviews in Economic Geology*, Vol. 7.
- WU F. Y., YE M. & ZHANG S. H. 1995. The geodynamic model of the Manzhouli-Suifenghe geoscience transect. *Earth Sciences* **20**, 535–9 (in Chinese with English abstract).
- WU F. Y., JAHN B. M., WILDE S. A. & SUN D. Y. 2000. Phanerozoic continental crustal growth: Sr-Nd isotopic evidence from the granites in northeastern China. *Tectonophysics* **328**, 87–113.
- WU F. Y., WILDE S. A. & SUN D. Y. 2001a. Zircon SHRIMP ages of gneissic granites in Jiamusi Massif, northeastern China (in Chinese with English abstract). *Acta Petrologica Sinica* **17**, 443–52.
- WU F. Y., SUN D. Y., LI H. M. & WANG X. L. 2001b. The nature of basement beneath the Songliao Basin in NE China: Geochemical and isotopic constraints. *Physics and Chemistry of the Earth (Part A)* **26**, 793–803.
- WU F. Y., SUN D. Y., LI H. M., JAHN B. M. & WILDE S. A. 2002. A-type granites in Northeastern China: Age and geochemical constraints on their petrogenesis. *Chemical Geology* **187**, 143–73.
- WU F. Y., JAHN B. M., WILDE S. A. *et al.* 2003. Highly fractionated I-type granites in NE China (I): Geochronology and petrogenesis. *Lithos* **66**, 241–73.
- WU F. Y., YANG J. H., WILDE S. A. & ZHANG X. O. 2005. Geochronology, petrogenesis and tectonic implications of the Jurassic granites in the Liaodong Peninsula, NE China. *Chemical Geology* **221**, 127–56.
- XIAO W. J., WINDLEY B., HAO J. & ZHAI M. G. 2003. Accretion leading to collision and the Permian Solonker suture, Inner Mongolia, China: Termination of the Central Asian Orogenic Belt. *Tectonics* **22**, 2002TC001484.
- YAN J. Y., TANG K. D., BAI J. W. & MO Y. C. 1989. High pressure metamorphic rocks and their tectonic environment in northeastern China. *Journal of South-eastern Asian Earth Sciences* **3**, 303–13.
- YE H. W. & ZHANG X. 1994. The  $^{40}\text{Ar}$ - $^{39}\text{Ar}$  age of the vein crossite in blueschist in Mudanjiang area NE China and its geological implication (in Chinese with English abstract). *Journal of Changchun University of Earth Sciences* **24**, 369–72.
- YE M., ZHANG S. H. & WU F. Y. 1994. The classification of the Paleozoic tectonic units in the area crossed by Manzhouli-Suifenghe geoscience transect (in

- Chinese with English abstract). *Journal of Changchun University of Earth Sciences* **24**, 241–5.
- YUAN H. L., GAO S., LIU X. M., LI H. M., GUNTHER D. & WU F. Y. 2004. Accurate U-Pb age and trace element determinations of zircon by laser ablation – Inductively Coupled Plasma Mass Spectrometry. *Geostandards and Geoanalytical Research* **28**, 353–70.
- ZAMORAS L. R. & MATSUOKA A. 2004. Accretion and postaccretion tectonics of the Calamian Islands, North Palawan block, Philippines. *Island Arc* **13**, 506–19.
- ZHANG X. Z. 1992. Heilongjiang melange: The evidence of Caledonian suture zone of the Jiamusi massif (in Chinese with English abstract). *Journal of Changchun University of Earth Sciences*, Special Issue: Doctoral Thesis. **22**, 94–101.
- ZHANG Y. B., WU F. Y., WILDE S. A., ZHAI M. G., LU X. P. & SUN D. Y. 2004. Zircon U-Pb ages and tectonic implications of ‘Early Paleozoic’ granitoids at Yanbian, Jilin province, NE China. *Island Arc* **13**, 484–505.
- ZHAO C. J., PENG Y. J., DANG Z. X. *et al.* 1996. *The Formation and Evolution of Crust in Eastern Jilin and Heilongjiang Provinces*. Liaoning University Press, Shenyang (in Chinese with English abstract).
- ZHOU X. M. & LI W. X. 2000. Origin of late Mesozoic igneous rocks in Southeastern China: Implication for lithospheric subduction and underplating of mafic magmas. *Tectonophysics* **326**, 269–87.
- ZONENSHAIN L. P., KUZMIN M. I. & KONONOV M. V. 1985. Absolute reconstructions of the Paleozoic oceans. *Earth and Planetary Science Letters* **74**, 103–16.
- ZYABREV S. & MATSUOKA A. 1999. Late Jurassic (Tithonian) radiolarians from a clastic unit of the Khabarovsk complex (Russian Far East): significance for subduction accretion timing and terrane correlation. *Island Arc* **8**, 30–7.